[ **Article ID**] 1003 - 6326( 2002) 06 - 1107 - 05

# Separation of inclusions from aluminum melt using alternating electromagnetic field <sup>10</sup>

LI Ke(李 克), WANG Jun(王 俊), SHU Da(疏 达), LI Tian-xiao(李天晓), SUN Bao-de (孙宝德), ZHOU Yao-he(周尧和)

(School of Materials Science and Engineering, Shanghai Jiaotong University, Shanghai 200030, China)

[Abstract] Effects of processing variables such as frequency of imposed magnetic field, imposed magnetic flux density, processing time, diameter of inclusions, and value of  $r_1/\delta$  on the electromagnetic separating (EMS) removal efficiency were analyzed theoretically. The higher the frequency, the wider the range of  $r_1/\delta$  will be. Removal efficiency reaches the maximum while  $r_1/\delta$  ranges from 1.5 to 2. And the experimental results on aluminum melt show that higher frequency and magnetic flux density make for higher removal efficiency, matching well with the theoretical results. When f is 15. 6 kHz,  $B_e$  is 0.1 T, and imposed time is 10 s, more than 80% inclusion particles with 6  $\mu$ m diameter can be removed.

[Key words] alternating electromagnetic field; aluminum melt; inclusion; EMS; removal efficiency

[CLC number] TG 146

[Document code] A

### 1 INTRODUCTION

Demands to the performance of aluminum alloy are higher than ever with its wide use in the field of car product, aircraft manufacturing and electric product. It is also well known that nonmetallic inclusions in the alloy not only form porosity, but also result in stress concentration and low plasticity and ductility<sup>[1]</sup>. Therefore, refining processing used on the melt is necessary to produce high quality alloy. Traditional processes, such as gravity sedimentation/flotation, degassing, flux refining and filtration, can hardly meet the cleanliness levels demanded in most applications due to their limitations on the low efficiency for the micrometer sized inclusions and making dirty to the environment<sup>[2]</sup>. Thus, a clean, effective and continuous process has become of great importance to meet the demand for cleaner metals.

Applications of electromagnetic separation techniques have been widely studied in recent years<sup>[3~5]</sup>. Compared with the other methods, AC magnetic field shows great advantages because it needs no loop circle for the imposed current and has no contaminative problem on the metal electrode. Furthermore, electromagnetic separation force can remove micrometer-sized inclusions in principle by using high-intensity force fields at almost constant rate<sup>[6]</sup>. The process of applying alternating electromagnetic field on the separation of inclusions from melt was first developed by El-Kaddah<sup>[7]</sup>, in whose design, the adjustments of the direction of imposing magnetic field and the magnetic flux density become eas-

ier. But due to the weak magnetic field in most area opposite to the coil, the removal efficiency is badly influenced<sup>[8]</sup>. The maneuverability of applying the electromagnetic field induced in a coil on the particle separation was theoretically demonstrated by Yamao et al<sup>[9]</sup>. Experiments on the aluminum melt were also investigated. But no accurate experimental results can be used to demonstrate the relation between various parameters and the removal efficiency.

In the present work, the authors investigate the effect of different processing parameter on the removal efficiency ( $^{\eta}$ ). The effect of external factors in the operating process on the practical efficiency is also discussed.

### 2 EXPERIMENTAL

High frequency magnetic field was generated by JGGCF  $50 \cdot 10/30$  induced heating power supply ( IG-BT). The magnetic flux density can be calculated as follows:

$$B_{e} = \frac{E}{4.44fNS} \tag{1}$$

AF3. 68 Sir 1. 72 Al $_2$ O $_3$  ( mass fraction, %), in which 6  $\mu$ m alumina particles act as simulative inclusions, is used as the original alloy. Schematic experimental apparatus is shown in Fig. 1. Firstly, separators with 4.5~ 10 mm diameter ceramic pipes were preheated to 300 °C and the power of IGBT was turned on. Then molten alloy at 750 °C was poured into the separator after being mixed. After presetting, the melt was left to solidify in the separator. The samples of the solidified

metal before and after processing were analyzed with LECO image analysis system to determine the inclusion content in the metal and the inclusion distribution across the section of the separator.

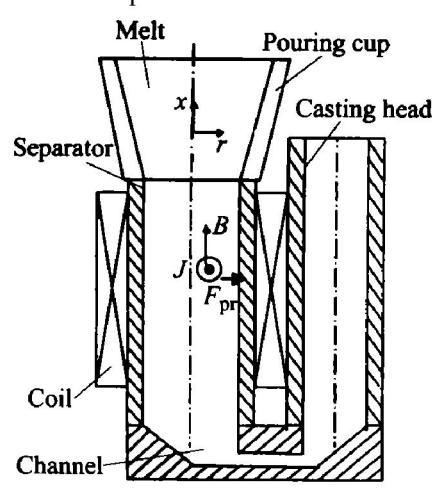


**Fig. 1** Schematic equipment for inclusion separation using alternating magnetic field

### 3 RESULTS AND DISCUSSION

#### 3. 1 Theoretical analysis of removal efficiency

In an infinitely long coil and melt, the electromagnetic force,  $F_{pr}$  imposed on per unit volume inclusion particle can be expressed as follows<sup>[6]</sup>:

$$F_{\rm pr} = -\frac{B_{\rm e}^2}{\sqrt{2}\,\mu_{\rm e}r_1} f^* \,(\,\xi\,R) \tag{2}$$

where

$$f^{*}(\xi R) = \xi I \operatorname{ber}_{0}(\xi R) (\operatorname{ber}_{1}(\xi R) + \operatorname{bei}_{1}(\xi R)) - \operatorname{bei}_{0}(\xi R) \cdot (\operatorname{ber}_{1}(\xi R) - \operatorname{bei}_{1}(\xi R))] / [\operatorname{ber}_{0}^{2} \xi + \operatorname{bei}_{0}^{2} \xi J]$$
(3)

According to the Stokes law, the terminal migration velocity,  $v_{\rm pr}$ , of the particles can be derived as

$$v_{\rm pr} = -\frac{d_{\rm p}^2}{24 \,\mu} \cdot F_{\rm pr} \tag{4}$$

By substituting Eqn. (4) into Eqn. (2), the terminal migration velocity can be obtained as

$$v_{\rm pr} = -\frac{d_{\rm p}^2 B_{\rm e}^2}{24\sqrt{2}\,\mu\mu_{\rm e} r_{\perp}} f^* \left(\xi R\right) \tag{5}$$

A special method was used to calculate the removal efficiency of electromagnetic separation in this condition<sup>[6]</sup>. Firstly, a non-dimensional radial coefficient is defined as

$$R_i = \frac{r}{r_1} \tag{6}$$

Due to the applied electromagnetic force, a spherical particle will experience a varying accelerated motion process, migrating from a position of  $R_i$  to the outer wall (R=1). The time when it arrives at the wall can be expressed by

$$t_i = r_1 \cdot \int_{R_i}^1 \frac{1}{v_{\text{pr}}} dR \tag{7}$$

By the time when  $t = t_i$ , all the particles located at the area where  $R > R_i$  will be moved to the wall and captured. Thus, the corresponding removal efficiency can be defined as

### 3. 2 Effect of $r_1/\delta$ on removal efficiency $\eta$

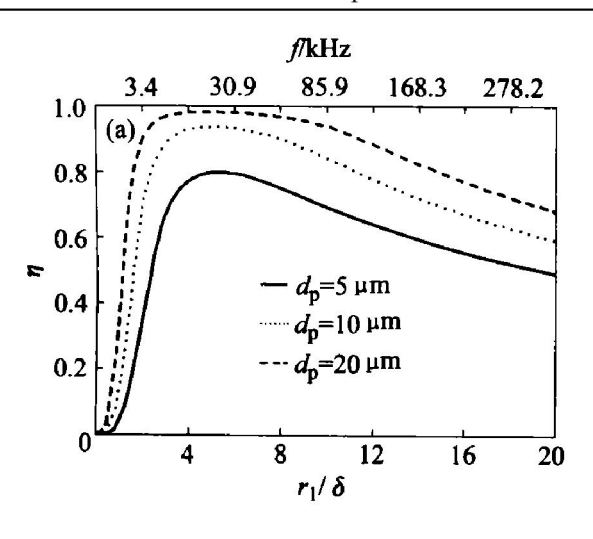
Fig. 2(a) shows the effect of  $d_{\rm p}$  on the relation between theoretical efficiency  $\Pi$  and  $r_{\rm 1}/\delta$  at constant  $r_{\rm 1}=5$  mm,  $B_{\rm e}=0.1$  T and t=10 s. As seen from the figure,  $\Pi$  increases with increasing  $d_{\rm p}$ , because  $v_{\rm pr}$  is proportional to the square of  $d_{\rm p}$ , as shown in Eqn. (5). The maximal value of  $\Pi$  increases rapidly with increasing  $r_{\rm 1}/\delta$  in the initial stage, but the rate of increasing becomes smaller as  $\Pi$  approaches unity. The value of  $\Pi$  reaches maximum when  $r_{\rm 1}/\delta$  is about  $2\sim 3$ . From the figure, we also found that the effective range of  $r_{\rm 1}/\delta$  becomes wider with increasing  $d_{\rm p}$ . For particles with diameter of  $20~\rm km$ , high value of  $\Pi$  can be obtained in the range from 10 to  $50~\rm kHz$ .

Fig. 3(a) shows the effect of frequency on the relation between the theoretical efficiency and  $r_1/\delta$  at four constant values of frequency, 5, 10, 20 and 40 kHz. It can be seen from the figure that there is the similar variation range of  $r_1/\delta$  to reach the maximal value of  $\mathfrak{I}$ , as shown in Fig. 2(a). The value of  $\mathfrak{I}$  reaches maximum when  $r_1/\delta$  is about  $1 \sim 3$  and decreases dramatically when  $r_1/\delta$  is larger than 3.

To achieve a desirable value of  $\mathfrak{I}$  for a certain inclusion size, the frequency f and the radius of the pipe  $r_1$  should be considered to the same extent. We chose two frequencies, 15. 6 kHz and 8. 3 kHz, in the experiments for the reason determined from Fig. 2(a). When the range of  $r_1/\delta$  is chosen as  $2\sim 3$  at 15. 6 kHz, the corresponding  $r_1$  ranges from 3. 5 to 4. 7 mm. The experimental results of electromagnetic separation on the arluminum melt are show in Table 1. The comparative

 Table 1
 Experimental results of processing

on aluminum melt						
Sample No.	d / mm	$B_{ m e}/{ m T}$	f/kHz	$r_1/\delta$	<i>t</i> /s	η %
1	10	0. 120	15.6	2. 131	300	100
2	10	0.120	15.6	2.131	60	100
3	10	0.120	15.6	2.131	30	99.6
4	10	0.120	15.6	2. 131	20	98.0
5	10	0.120	15.6	2.131	5	61.0
6	4. 5	0.120	15.6	0.959	10	81.0
7	6.0	0.120	15.6	1.279	10	93.7
8	8.0	0.120	15.6	1.705	10	95. 1
9	10	0.120	15.6	2. 131	10	98.5
10	4. 5	0. 175	8.3	0.700	10	53.5
11	6.0	0. 175	8.3	0.933	10	89.6
12	8.0	0. 175	8.3	1.244	10	91.5
13	10	0. 175	8.3	1.555	10	94.0



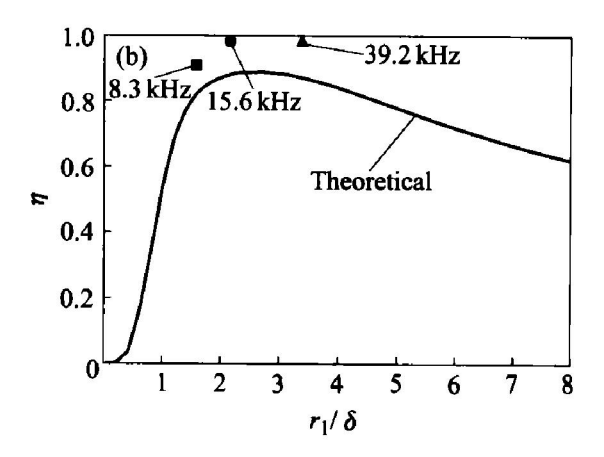
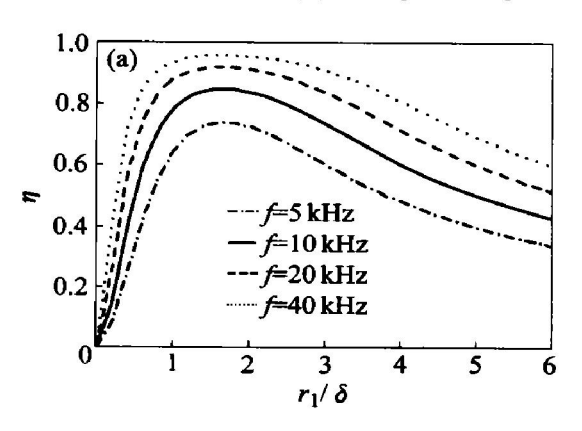


**Fig. 2** Effect of  $r_1/\delta$  on removal efficiency with constant pipe diameter

$$(t=10 \text{ s}, r_1=5 \text{ mm}, B_e=0.12 \text{ T})$$

(a) Theoretical  $\eta$  with different  $d_p$ ;

(b) —Comparison of practical  $\Pi$  with theoretical  $\Pi$  while  $d_p$  is 6  $\mu$ m



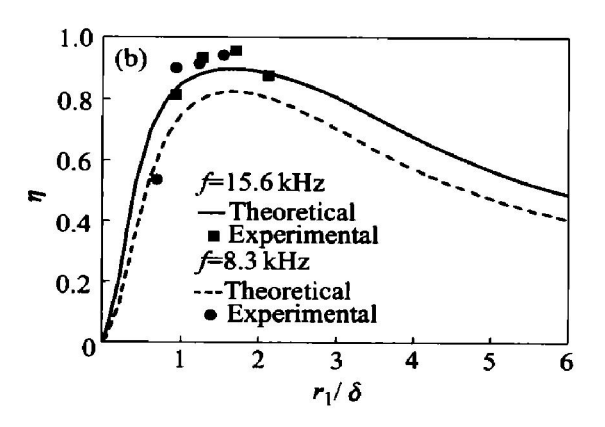


Fig. 3 Effect of  $r_1/\delta$  on removal efficiency with constant frequency  $(d_p = 6 \text{ } \text{Pm}, \ t = 10 \text{ s}, \ B_e = 0.12 \text{ T})$ 

(a) —Theoretical  $\eta$  at different frequency; (b) —Comparison of practical  $\eta$  with theoretical  $\eta$ 

curves between practical  $\Pi$  and theoretical  $\Pi$  were described in Fig. 2(b) and Fig. 3(b), in which we found that the experimental values of  $\Pi$  match well with the calculated curves.

# 3. 3 Effect of magnetic flux density on removal efficiency

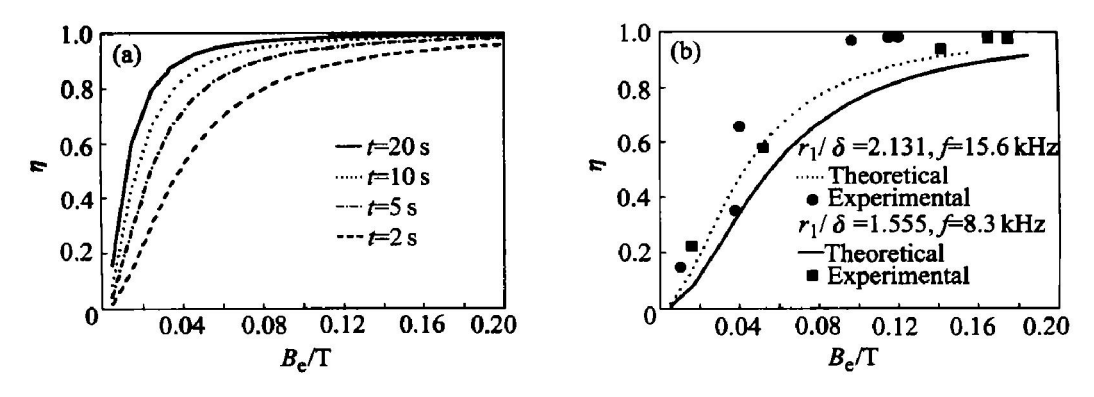
Fig. 4(a) shows the effect of magnetic flux density on the theoretical removal efficiency with four different processing times. As seen from the figure, the value of  $\Pi$  increases remarkably with increasing value of  $B_e$  when the processing time is longer. The practical efficiency at 15. 6 kHz and 8. 3 kHz are obtained respectively, as shown in Fig. 4(b). Results show that the practical removal efficiency is very close to the theoretical value when the value of  $B_e$  is larger than 0. 1 T, but is lower than the theoretical value at the small value of  $B_e$ . Accordingly, the removal efficiency at the two frequencies is above 90% when the value of  $B_e$  is larger than 0. 1 T. With decreasing  $B_e$ , the value of  $\Pi$  decreases dramatically, which indicates that in order to obtain high re-

moval efficiency, higher magnetic flux density should be imposed.

The macroscopic photo of the longitudinal cutting sample in the circular pipe separator and the metallograph of the local area in the sample are shown in Fig. 5. It can be seen from the figure that most of the inclusions congregate at the side of the wall and concentrate in the center of the coil. Obviously, the removal efficiency is very small at two outlets of the coil where the magnetic density is lesser than the central part. Furthermore, due to the asymmetrical distribution of magnetic field in the coil, unstable eddy flow is generated<sup>[3]</sup>, which is extremely strong at the end of the coil, and the removal efficiency is badly influenced consequently. Therefore, further investigation should be made to manifest the negative effect of this kind of disturbed flow on the electromagnetic separation<sup>[10]</sup>.

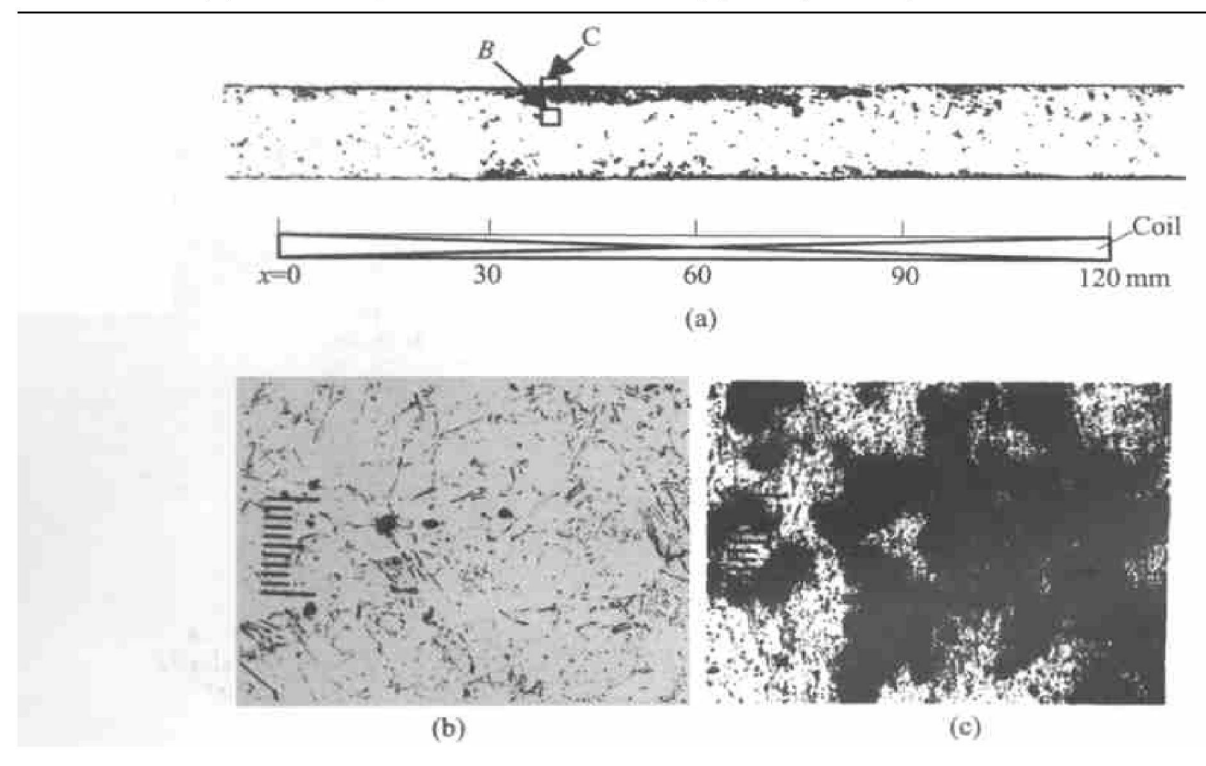
### 3. 4 Effect of imposing time on removal efficiency

Fig. 6(a) shows the effect of imposing time on the theoretical efficiency at three values of  $B_{\rm e}$ . With increasing processing time the value of  $\eta$  in



**Fig. 4** Relation between removal efficiency and magnetic flux density ( $d_p = 6 \, \mu_m$ ,  $t = 10 \, \text{s}$ ,  $r_1 = 5 \, \text{mm}$ )

(a) —Effect of  $B_e$  on theoretical  $\P$  at 15.6 kHz; (b) —Comparison of practical  $\P$  with theoretical  $\P$ 



**Fig. 5** Macroscopical photo(a) of longitudinal cutting sample in circular pipe separator and metallograph of area B(b) and C(c) (Al-3. 68% Si-1. 72% Al<sub>2</sub>O<sub>3</sub>,  $r_1$ = 3 mm,  $B_c$ = 0. 12 T, f= 15. 6 kHz, t= 10 s)

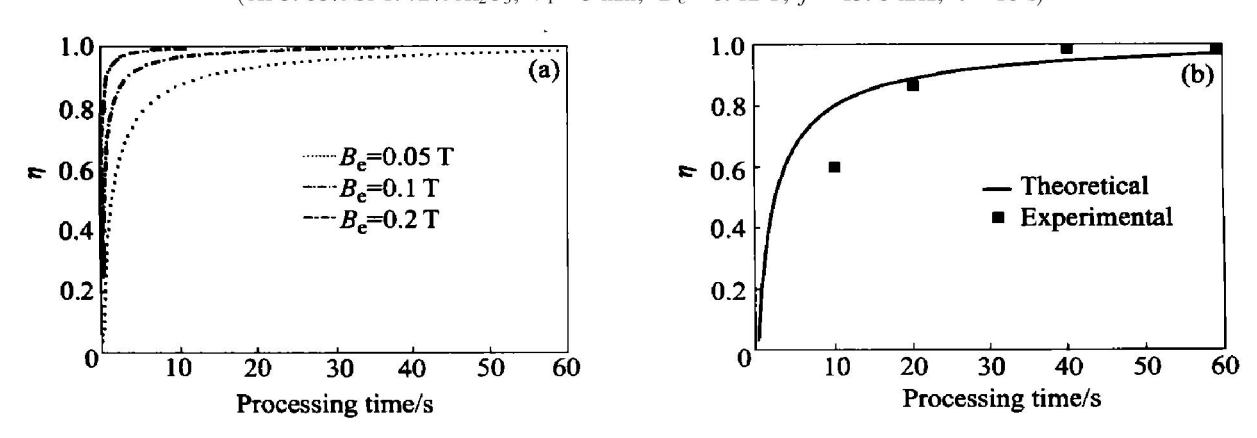


Fig. 6 Relation between removal efficiency and processing time( $d_p$ = 6  $\mu$ m,  $r_1$ = 5 mm, f= 15. 6 kHz)

(a) —Effect of t on theoretical  $\eta$ ; (b) —Comparison of practical  $\eta$  with theoretical  $\eta$  at 0. 12 T

creases rapidly. And the removal efficiency of more than 80% can be obtained after processing 10 s at 0.1 T.

Meanwhile a series values of  $\,^{n}$  were measured at 0.12 T, as shown in Fig. 6(b). It can be seen from the

figure that the practical ¶ match well with the result of theoretical analysis. Higher efficiency reaching 100% can be obtained when the processing time is extended to 30 s. Nevertheless, it is totally unreasonable if the flowing melt was treated so long time in the continuous treatment of the practical industrial manufacture.

## 4 CONCLUSIONS

- 1) Theoretical analysis indicated that the higher frequency of the alternating electromagnetic field, the wider the numeric range of  $r_1/\delta$  will be. Normally, EMS removal efficiency reaches the maximum while  $r_1/\delta$  ranges from 1.5 to 2.
- 2) The experimental results match well with the result of theoretical analysis while  $B_{\rm e}$  is larger than 0.1 T. Higher frequency and magnetic flux density make for higher removal efficiency. Higher efficiency can be obtained in the case that f is 15.6 kHz than that of 8.3 kHz. While  $B_{\rm e}$  is 0.1 T, and imposed time is 10 s, more than 80% inclusion particles with 6  $\mu$ m diameter can be removed from the melt.

### **Nomenclatures**

 $B_{\rm e}$  —Effective magnetic flux density, T;

 $ber_n$ ,  $bei_n$ —The nth order Kelvin functions;

 $d_{\rm p}$  —Diameter of particles,  $\mu_{\rm m}$ ;

E —Effective induced electromotive force in the measuring coil, V;

 $F_{pr}$ —Root-mean-square value of pinch force exerted on particle, N;

f —Frequency of magnetic field, kHz;

N —Turns of the measuring coil;

R — Nondimensional radial distance,  $R = r/r_1$ ;

r —Radial distance, mm;

 $r_1$ —Radius of circular pipe, mm;

S —Effective area of the measuring coil,  $m^2$ ;

t—Processing time, s;

s;

 $v_{\rm pr}$  —Terminal radial migration rate of particle, m/

µ—Kinetic viscosity of melt, pa•s;

μ<sub>e</sub> —Magnetic permeability of melt, H/m;

n-Removal efficiency of particles;

 $\delta$ —Skirr effect depth  $\delta = \sqrt{2/\mu_e} \sigma_f \omega$ , mm;

of Electrical conductivity of melt, S/m;

 $\xi$ —Nondimensional factor  $\xi = \sqrt{2r_1/\delta}$ ;

ω—Angular frequency, rad/s

### [REFERENCES]

- Peterson R D. Common Impurities in Aluminum Alloys[A].
   Proceedings of 3rd International Conference on Aluminum Processing [C]. Paris, 1994. 75.
- [2] Eckert C E. Inclusions in aluminum foundry alloys [J]. Modern Casting, 1991, 4: 28 - 30.
- [3] Taniguchi S, Brimacombe J K. Application of pinch force to the separation of inclusion particles from liquid steel[J]. ISIJ Int, 1994, 34(9): 722 - 731.
- [4] LI Tiarr xiao, XU Zherr ming. Physical simulation and theoretical analysis of migrating rate of inclusions in aluminum melt in electromagnetic field[J]. Trans Nonferrous Met Soc China, 2001, 11(1): 30 34.
- [5] ZHONG Yurr bo, REN Zhong ming. Separation of inclusions from liquid metal contained in a triangle/square pipe by traveling magnetic field[J]. Trans Nonferrous Met Soc China, 2000, 10(2): 240 245.
- [6] SHU Da, SUN Bao de. Study of electromagnetic separation of nonmetallic inclusions from aluminum melt[J]. Metall Mater Trans A, 1999, 30A: 2979.
- [7] El-Kaddah N. A Comprehensive Mathematical Model of Electromagnetic Separation of Inclusion in Molten Metals [A]. IEEE on Industrial Applications [C]. New York, 1988. 1162.
- [8] El-Kaddah N, Patel A D, Natarajan T T. The electromagnetic filtration of molten aluminum using an induced current separator [J]. JOM, 1995, 49: 46.
- [9] Yamao F, Sassa K. Separation of inclusions in liquid metal using fixed alternating magnetic field[J]. Tetsur to Hagane, 1997, 83: 30.
- [10] Park J P, Morihira A. Elimination of non-metallic inclusions using electromagnetic force [J]. Tetsur-to-Hagane, 1994, 80: 31.

(Edited by PENG Chao qun)